RESEARCH ARTICLE

Morphological Changes of Porcine Granulosa Cells during *in vitro* Expansion

Hoang Nghia Son[1,2], Ho Nguyen Quynh Chi[1,2] and Le Thanh Long[1,2,*]

[1]Animal Biotechnology Department, Institute of Tropical Biology, Vietnam Academy of Science and Technology, *9/621 Hanoi highway*, Linh Trung Ward, Thu Duc District, Ho Chi Minh City 700000, Vietnam; [2]Graduate University of Science and Technology, Vietnam Academy of Science and Technology, 18 Hoang Quoc Viet, Cau Giay District, Ha Noi 100000, Vietnam
*Corresponding author: lelongvast@gmail.com

A B S T R A C T

This study aimed to assess morphological changes of porcine granulosa cells (pGCs) following *in vitro* long-term culture. The pGCs from passage 5 showed a dramatic enlargement of cytoplasm (14422.600 ± 1300.704 μm^2) which was 8.23-fold higher than pGCs from primary culture (1752.100 ± 102.244 μm^2). Nuclear areas were increased from passage 0 (164.990 ± 3.461 μm^2) to passage 4 (399.514 ± 15.110 μm^2) and passage 5 (416.326 ± 32.683 μm^2), respectively. The nucleocytoplasmic ratio of pGCs from passage 0 was 0.089 ± 0.002 which was 2-fold higher than passage 4 (0.045 ± 0.002) and 3-fold higher than passage 5 (0.029 ± 0.002). The diameter of microfilament bundles of pGCs was increased from passage 0 (1.171 ± 0.031 µm) to passage 4 (1.550 ± 0.056 µm) and passage 5 (1.579 ± 0.053 µm), respectively. The weak expression of beta-galactosidase was observed in the several pGCs from passage 2, while pGCs from passage 4 showed the strong activity of beta-galactosidase. The flow cytometry analysis demonstrated that the ratio of apoptotic pGCs was increased through in vitro expansion. These results revealed that pGCs exposed replicative senescent characteristics including the increase of nuclear and cell size, as well as the increase of diameter of actin filament bundles in cytoplasm, and the reduction of nucleocytoplasmic ratio.

To Cite This Article: Son HN, Chi HNQ and Long LT, 2020. Morphological changes of porcine granulosa cells during *in vitro* expansion. Pak Vet J. http://dx.doi.org/10.29261/pakvetj/2020.010

INTRODUCTION

Senescence is considered to be the endpoint for dividing cells (Campisi and d'Adda di Fagagna, 2007; Chen *et al.*, 2013). The recent studies hypothesized that senescence can be demonstrated as a highly dynamic, multi-step process. The senescent characteristics evolve and diversify as tumorigenesis, but without proliferation (Wang *et al.*, 2011; De Cecco *et al.*, 2013; Ivanov *et al.*, 2013). Senescent cells expose the loss of regenerative capacity which correlates to the reduction of tissue function (Campisi & d'Adda di Fagagna, 2007). One of the most important biomarkers of cellular senescence is stopping cell division, but cellular metabolism is carried out for a long time (Goldstein, 1990; Campisi & d'Adda di Fagagna, 2007). The other morphological biomarkers, which associate with senescent cells, include the increase of cell and nuclear size, number of multinucleated cells, numbers of microfilament bundles in cytoplasm, and the number of vacuoles in cytoplasm (Cristofalo and Pignolo, 1993; Leikam *et al.*, 2015).

During folliculogenesis, the granulosa cells provide a microenvironment to support oocyte development (Dumesic *et al.*, 2015). The transcriptional activity and the post-transcriptional modification of some proteins in oocytes were regulated by granulosa cells (Carabatsos *et al.*, 2000). Several observations supported that aging granulosa cells could also enhance oocyte aging. Thus, the oocyte quality can be negatively affected by degenerating granulosa cells. The previous studies demonstrated aging characteristics of granulosa cells. During the aging, an increase of apoptosis ratio was observed in granulosa cells (Sadraie *et al.*, 2000; Hui *et al.*, 2017; Fan *et al.*, 2019). The aging granulosa cells exposed a low genomic global DNA methylation and proliferative reduction (Goto *et al.*, 2013). However, morphologic modifications of pGCs during replicative senescence have been still unclear. Thus, the purpose of this study was to use pCGs as an *in vitro* model to estimate the replicative senescence including the changes in cell cycles, nucleocytoplasmic ratio, and diameter of microfilament bundles.

MATERIALS AND METHODS

Cell culture: Porcine ovaries were collected from the abattoir and transported to the laboratory in 3 hours. The porcine follicles were obtained by dissection and removed completely the blood and extra tissue by washing with PBS (Phosphate-buffered saline). Aspiration method was applied to achieve the fresh porcine granulosa cells (pGCs) from these above follicles. The medium for cell culture is Dulbecco's Modified Eagle Medium (Gibco, Germany) supplemented with 10% fetal bovine serum (Gibco, Germany) and 1% Pen/Strep (Gibco, Germany) and subcultured when the cells reach 80% confluence.

Actin filament staining: The 4% paraformaldehyde (Nacalai, Japan) was applied to fix pGCs at room temperature for 15 min, then the permeabilization of pGCs was carried out with 0.1% Triton X-100 in PBS (Merck, Germany) at room temperature for 1 hour. The pGCs were incubated with 1X Phalloidin CruzFluor™ 488 Conjugate (Santa Cruz Biotechnology, United States) for 1 hour and stained with 4',6-Diamidino-2-phenylindole dihydrochloride (Sigma, United States) for 30 min. The pGCs were gently rinsed with PBS 3 times for each step. The pGCs were observed under Cytell microscope (GE Healthcare, United States) to estimate the morphology of cell and nuclear.

Area measurement: The cell and nuclear area, and the diameter of microfilament bundle were measured by ImageJ software (National Institutes of Health, Bethesda, MD). The figures were converted to grayscale (type 8 bit) then the background noise and autofluorescence were removed by adjusting to the threshold function. The outline of cell and nuclear is automatically drawn and the area measurement was subsequently carried out.

β-Galactosidase assay: The beta-Galactosidase Detection Kit (ab102534, Abcam, United States) was employed to assess the expression of β-Galactosidase in pGCs. The pGCs were fixed with 0.5 mL of Fixative Solution for 15 min at room temperature, then incubated overnight at 37°C with 0.5 mL Staining Solution Mix. The pGCs were washed twice with cold PBS for each step. The expression of β-Galactosidase in pGCs was evaluated under microscope by the development of blue color.

Flow cytometry analysis: The pGCs were harvested and adjusted cell suspension to a concentration of 1 x 10^6

cells/mL in 100 µL 1X Binding Buffer. The pGCs were incubated with 5 µL of FITC Annexin V and 5 µL PI (The Apoptosis Detection Kit I, BD Biosciences, United States) for 15 min at RT in the dark. The cell cycle and apoptosis of pGCs were assessed by BD Accuri C6 Plus (BD Biosciences, United States).

Statistical analysis: Statistical analysis was performed by one-way ANOVA. The data were represented as means± SEM. The p-value less than 0.05 is considered statistically significant.

RESULTS

The pGCs were *in vitro* expanded from primary culture (passage 0) to passage 6. pGCs area was increased from passage 0 (1752.100±102.244 µm²) to passage 4 (8743.821±512.882 µm²) (Table 1). The pGCs from passage 5 showed a drastic enlargement of cytoplasmic area (14422.600±1300.704 µm²) which was 8.23-fold higher than cell from primary culture.

The nuclear areas of pGCs from different passages were demonstrated in Table 1. Nuclear areas were increased from passage 0 (164.990±3.461 µm²) to passage 4 (399.514±15.110 µm²) and passage 5 (416.326±32.683 µm²), respectively. However, there was no significant difference between passage 4 and passage 5 in nuclear area. Fig. 1 showed nuclear morphologic modification of pGCs from different passages. The nuclear shape of pGCs from passage 0 was small, homogenous, and circular. The nuclear area enlargement induced the deformation of nuclear shape in pGCs from passage 4 and passage 5.

The nucleocytoplasmic ratio (nuclear area/cell area) was also applied to estimate morphologic modification of pGCs during *in vitro* culture. In the contract to an increase of cell and nuclear area, pGCs showed a reduction of nucleocytoplasmic ratio (Table 1). The nucleocytoplasmic ratio from passage 0 was 0.089±0.002 which was 2-fold higher than passage 4 (0.045±0.002) and 3-fold higher than passage 5 (0.029±0.002).

**Table 1:** The changes of size parameters of cell, nuclear and microfilament bundle during *in vitro* expansion

|	P0	P4	P5
Cell area (µm²)	1752.100± 102.244[a]	8743.821± 512.882[b]	14422.600± 1300.704[c]
Nuclear area (µm²)	164.990± 3.461[a]	399.514± 15.110[b]	416.326±32.683[b]
Nucleocytoplamic ratio	0.089±0.002[b]	0.045±0.002[b]	0.029±0.002[c]
Microfilament bundle diameter (µm)	1.171±0.031[a]	1.550±0.056[b]	1.579±0.053[b]

a, b, c: statistically significant difference (P<0.05).


Fig. 1: The morphological changes of nuclear in pGCs during *in vitro* expansion. A, B, C: nuclear in pGCs from the passage 0, passage 4, and passage 5. Nuclear was stained with DAPI (single color). Scale bar = 223.64 µm.
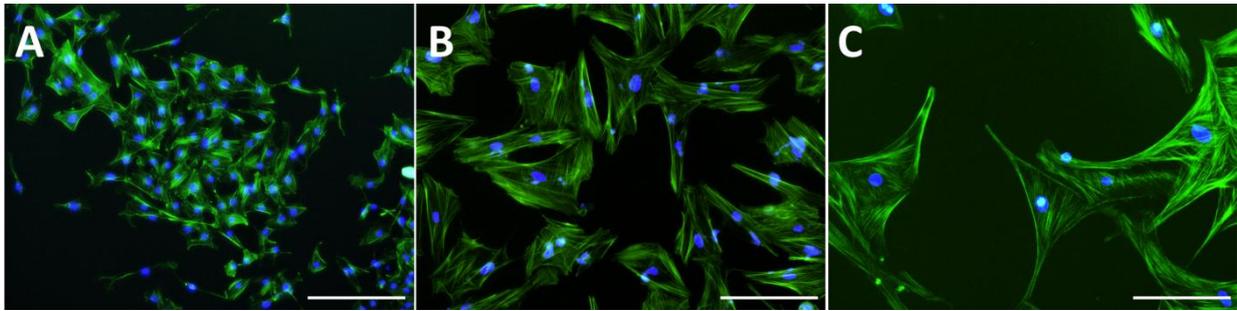
Fig. 2: The morphological changes of pGCs during *in vitro* expansion. A, B, C: pGCs from the passage 0, passage 4, and passage 5. Actin filament was stained with Phalloidin CruzFluor™ 488 Conjugate (green) and nuclear was stained with DAPI (blue). Scale bar = 223.64 µm.
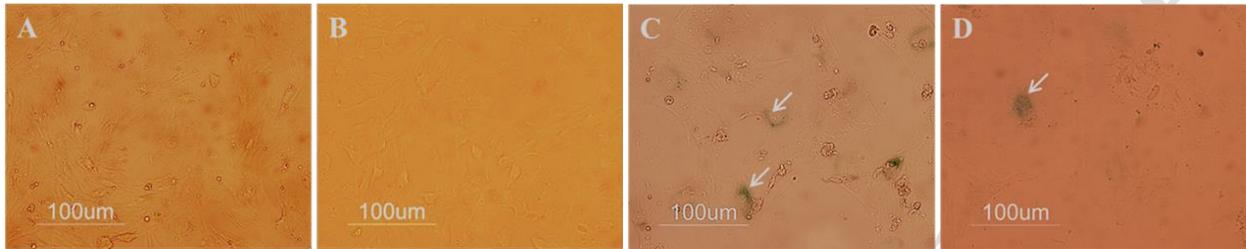
Fig. 3: Senescence-associated beta-galactosidase staining. A, B, C, D: pGCs from primary culture, passage 2, passage 4, and passage 6 (200X total magnification).
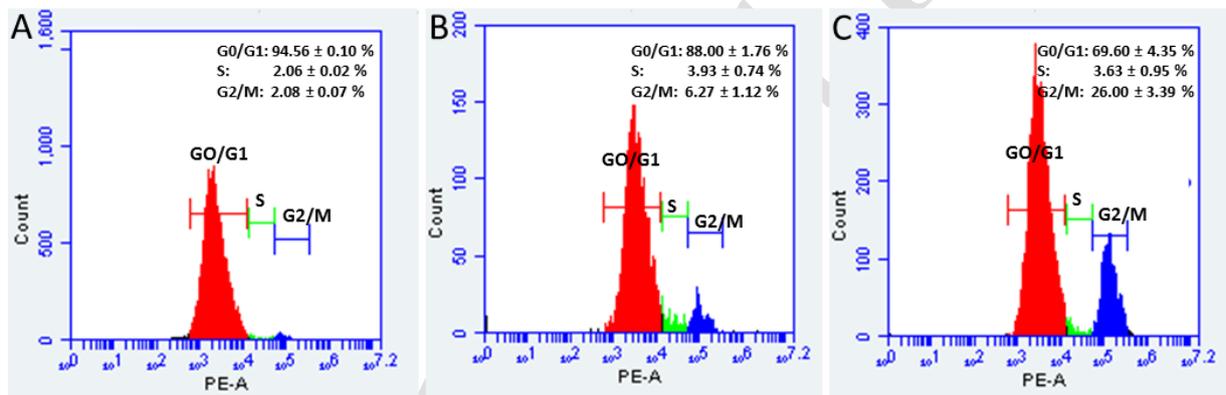
Fig. 4: Flow cytometry analysis of cell cycle in pGCs. A, B, C: cycle distributions of pGCs from the primary culture, passage 2, passage 4.
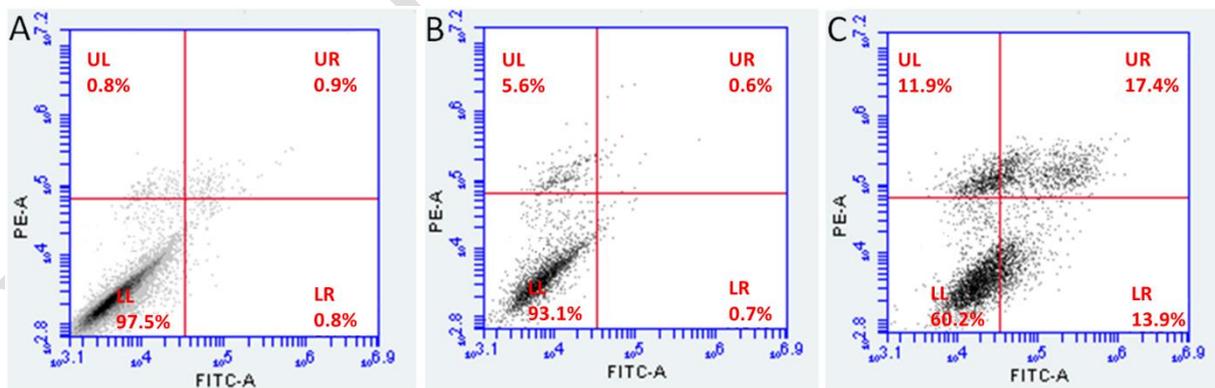
Fig. 5: Flow cytometry analysis of apoptotic pGCs. A, B, C: cycle distributions of pGCs from the primary culture, passage 2, passage 4.

The pGCs of passage 0 retained the homogeneous morphology. The polymorphotype of pGCs from passage 4 and passage 5 was caused by the enlargement of cytoplasm, leading to the various levels of lobation in cytoplasm (Fig. 2). The cytoplasmic enlargement is correlated to modification of cytoskeleton system, especially microfilament. The diameter of microfilament bundles of pGCs was increased from passage 0 (1.171 ± 0.031 µm) to passage 4 (1.550 ± 0.056 µm) and passage 5 (1.579 ± 0.053 µm), respectively. However, there was no significant difference between passage 4 and passage 5 in diameter of microfilament bundles.

The pGCs from primary culture, passage 2, passage 4 and passage 6 were used for estimating beta-galactosidase

expression. The result showed that the negative staining of beta-galactosidase was observed in pGCs from primary culture and passage 2 (Fig. 3A, 3B). The dark green color areas were appeared in pGCs from passage 4, revealing the expression of beta-galactosidase in these cells (Figure 3C). Fig. 3D showed pGCs from passage 6 with a strong positive stain of beta-galactosidase.

The pGCs from primary culture, passage 2, and passage 4 were used to estimate the cell cycle by flow cytometry analysis (Fig. 4). The pGCs from primary culture showed the highest ratio in G0/G1 phase (94.56±0.10%). The cell ratio in G0/G1 phase was reduced through the in vitro expansion. The pGCs ratio in G0/G1 phase from passage 2 (88.00±1.76%) and passage 4 (69.60±4.35%) was lower than primary culture. In this study, we also assessed the changes of apoptotic ratio in pGCs from primary culture to passage 4 (Fig. 5). There was no statistically significant difference of apoptotic pGCs ratio between primary culture (1.7±0.04%) and passage 2 (1.3±0.32%). However, the ratio of apoptotic pGCs from passage 4 (31.3±2.32%) was significantly increased, comparing to other previous passages (P<0.05).

DISCUSSION

In this study, the pGCs were expanded through to six passages and showed several morphological changes comprising the cell and nuclear enlargement, the formation of large actin filament bundles, and a reduction of nucleocytoplasmic ratio. These modifications were senescent characteristics during *in vitro* culture (Cho *et al.*, 2004). The pGCs from passage 5 were huge enlarged than pGCs from early passages, suggesting that the morphological modification was occurred in pGCs during *in vitro* expansion. This modification is one of the most important biomarkers in replicative senescence (Sikora *et al.*, 2016; Herranz and Gil, 2018).

There is a correlation between cell and nuclear area increase. Nuclear size was modulated by nuclear components such as nucleolus, enzymes, macromolecules (Miyoshi and Sugimoto, 2008; Webster *et al.*, 2009). One of the most important components of nuclear is genome, however, genomic size has no effect on nuclear size (Webster *et al.*, 2009). It suggests that the cytoplasmic volume is more important than DNA content in determining nuclear size, and the larger expansion of cytoplasm induces a stronger transcription in nuclear (Webster *et al.*, 2009). In the present study, an increase of nuclear area was observed in pGCs that could give a rise to transcription in larger cells (Webster *et al.*, 2009). The cytoplasmic enlargement relates to the process of *in vitro* aging (Neurohr *et al.*, 2019). The pGCs from late passages (passage 4 and passage 5) showed a low proliferation comparing to pGCs from primary culture (passage 0). The cytoplasmic expansion induced a reorganization and enhancement of actin microfilament bundles in pGCs (Moujaber *et al.*, 2019; Biran *et al.*, 2019). The microfilament bundles were displayed in multiple array networks which extended through the length of pGCs. Moreover, the diameter of microfilament bundles was increased in pGCs which exposed senescent characteristics. Thus, microfilament bundle extension could be proposed as a marker for replicative senescence.

The change of nucleocytoplasmic ratio is associated to the enlargement of cellular and nuclear area (Son *et al.*, 2019). It has been considered that the nucleocytoplasmic ratio plays an important factor for the cell cycle modulation (Slater *et al.*, 2005; Roca-Cusachs *et al.*, 2008). A measure of nucleocytoplasmic ratio is considered as a good indicator to estimate senescent state of cells population (Filippi-Chiela *et al.*, 2012). Under *in vitro* condition, the value of nucleocytoplasmic ratio is proximately 10% (Filippi-Chiela *et al.*, 2012). The present study demonstrated a dramatic reduction of nucleocytoplasmic ratio of pGCs from passage 0 (8.9%) to passage 5 (2.9%). This revealed that pGCs exposed a stronger enlargement in cytoplasm than nuclear which induced a decrease in nucleocytoplasmic ratio value.

Conclusions: The present study showed that the replicative senescence was observed in pGCs from long-term culture, demonstrated by modifications of cell areas and microfilament. The replicative senescence also induced the beta-galactosidase expression and the increase of the ratio of apoptotic pGCs.

REFERENCES

Biran A, Perelmutter M, Gal H, et al., 2019. Senescent cells communicate via intercellular protein transfer. Gen Develop 29:791-802.
Campisi J and d'Adda di Fagagna F, 2007. Cellular senescence: when bad things happen to good cells. Nat Rev Mol Cell Biol 8:729-40.
Carabatsos MJ, Sellitto C, Goodenough DA, et al., 2000. Oocyte-granulosa cell heterologous gap junctions are required for the coordination of nuclear and cytoplasmic meiotic competence. Dev Biol 226:167-79.
Chen H, Li Y, Tollefsbol TO, 2013. Cell Senescence Culturing Methods. Methods Mol Biol 1048:1-10.
Cho KA, Ryu SJ, Oh YS, et al., 2004. Morphological Adjustment of Senescent Cells by Modulating Caveolin-1 Status. J Biol Chem 279:42270-8.
Cristofalo VJ and Pignolo RJ, 1993. Replicative senescence of human fibroblast-like cells in culture. Physiol Rev 73:617-38.
De Cecco M, Criscione SW, Peckham EJ, et al., 2013. Genomes of replicatively senescent cells undergo global epigenetic changes leading to gene silencing and activation of transposable elements. Aging Cell 12:247-56.
Dumesic DA, Meldrum DR, Katz-Jaffe MG, et al., 2015. Oocyte environment: follicular fluid and cumulus cells are critical for oocyte health. Fertil Steri 103:303-16.
Fan Y, Chang Y, Wei L, et al., 2019. Apoptosis of mural granulosa cells is increased in women with diminished ovarian reserve. J Assist Reprod Genet 36:1225-35.
Filippi-Chiela EC, Oliveira MM, Jurkovski B, et al., 2012. Nuclear Morphometric Analysis (NMA): Screening of Senescence, Apoptosis and Nuclear Irregularities. PLoS One 7:1-10.
Goldstein S, 1990. Replicative senescence: the human fibroblast comes of age. Science 249:1129-33.
Goto H, Iwata H, Takeo S, et al., 2013. Effect of bovine age on the proliferative activity, global DNA methylation, relative telomere length and telomerase activity of granulosa cells. Zygote 21:256-64.
Herranz N and Gil J, 2018. Mechanisms and functions of cellular senescence. J Clin Invest 128:1238-46.
Hui L, Shuangshuang G, Jianning Y, et al., 2017. Systemic analysis of gene expression profiles in porcine granulosa cells during aging. Oncotarget 8:96588-603.
Ivanov A, Pawlikowski J, Manoharan I, et al., 2013. Lysosome-mediated processing of chromatin in senescence. J Cell Biol 202:129-43.

Leikam C, Hufnagel AL, Otto C, *et al.*, 2015. In vitro evidence for senescent multinucleated melanocytes as a source for tumor-initiating cells. Cell Death Dis 6:1-13.

Miyoshi D and Sugimoto N, 2008. Molecular crowding effects on structure and stability of DNA. Biochimie 90:1040-51.

Moujaber O, Fishbein F, Omran N *et al.*, 2019. Cellular senescence is associated with reorganization of the microtubule cytoskeleton. Cell Mol Life Sci 76:1169-83.

Neurohr GE, Terry RL, Lengefeld J, *et al.,* 2019. Excessive cell growth causes cytoplasm dilution and contributes to senescence. Cell 176:1083-97.

Roca-Cusachs P, Alcaraz J, Sunyer R, *et al*., 2008. Micropatterning of single endothelial cell shape reveals a tight coupling between nuclear volume in G1 and proliferation. Biophys J 94:4984-95.

Sadraie SH, Saito H, Kaneko T, *et al*., 2000. Effects of aging on ovarian fecundity in terms of the incidence of apoptotic granulosa cells. J Assist Reprod Genet 17:168-73.

Sikora E, Mosieniak G and Sliwinska MA, 2016. Morphological and functional characteristic of senescent cancer cells. Current Drug Targets 17:377-87.

Slater DN, Rice S, Stewart R, *et al*., 2005. Proposed Sheffield quantitative criteria in cervical cytology to assist the grading of squamous cell dyskaryosis, as the British Society for Clinical Cytology definitions require amendment. Cytopathology 16:179-92.

Son HN, Chi HNQ, Chung DC, *et al.*, 2019. Morphological changes during replicative senescence in bovine ovarian granulosa cells. Cell Cycle 18:1490-7.

Wang J, Geesman GJ, Hostikka SL, *et al*., 2011. Inhibition of activated pericentromeric SINE/Alu repeat transcription in senescent human adult stem cells reinstates self-renewal. Cell Cycle 10:3016-30.

Webster M, Witkin KL and Cohen-Fix O, 2009. Sizing up the nucleus: nuclear shape, size and nuclear-envelope assembly. J Cell Sci 122:1477-86.